Optics Communications 282 (2009) 2062–2065

Contents lists available at ScienceDirect

Optics Communications

journal homepage: www.elsevier.com/locate/optcom

Remote sensing of trace methane using mobile femtosecond laser system of *T&T Lab*

Y. Kamali [a,*], J.-F. Daigle [a], F. Théberge [b], M. Châteauneuf [b], A. Azarm [a], Y. Chen [a], C. Marceau [a], S.C. Lessard [a], F. Lessard [a], G. Roy [b], J. Dubois [b], S.L. Chin [a]

[a] Department of Physics, Engineering Physics and Optics and Center for Optics, Photonics and Laser (COPL), Laval University, Quebec City, QC, Canada G1V 0A6
[b] Defence Research and Development Canada-Valcartier, Quebec, QC, Canada G3J 1X5

ARTICLE INFO

Article history:
Received 22 December 2008
Received in revised form 2 February 2009
Accepted 2 February 2009

ABSTRACT

The mobile femtosecond laser facility T&T (terawatt & terahertz) of DRDC-Valcartier was used to detect trace methane gas remotely in an open field atmosphere during daytime (with strong sun light) using filament-induced fluorescence spectroscopy. Comparison of the results obtained in the laboratory and in the field validates the long range extrapolations of short distance results taken in our laboratory in the past. This could be considered a breakthrough for remote sensing based on filamentation.

1. Introduction

Advances in the propagation of intense femtosecond laser pulses in air have shown that the laser pulse self-focuses to form filaments and self-transforms into a white-light laser pulse or supercontinuum (SC) [1,2]. The high intensity inside the filament core ionizes the atmospheric molecules and produces a low density plasma ($\sim 10^{16}$ cm^{-3}) [3–6], which in turn defocuses the laser pulse. The balance between the self-focusing and defocusing limits the intensity in the filament zone to about 5×10^{13} W/cm^2 in air [1,2,7]. This is referred to as the intensity clamping [8–10]. With this high intensity, most molecules would be ionized and dissociated into excited fragments, which emit fluorescence. Such unique features of the filament-induced fluorescence molecular spectra were successfully used for the detection of gaseous molecules in our laboratory such as nitrogen [11,12], halocarbons [13], methane (CH_4) [14] and acetylene (C_2H_2) [15]. The application of filament-induced fluorescence to remote sensing of nitrogen [16] and ethanol in air [17] in combination with the traditional techniques of fluorescence spectroscopy and LIDAR (LIght Detection And Ranging) have been successfully tested. However, all these tests have been performed in a laboratory environment; outdoor remote sensing of gaseous pollutants using filamentation induced fluorescence in air has not been reported so far.

Methane is a dominant atmospheric pollutant and is of major importance in many environmental issues such as greenhouse effect and stratospheric ozone depletion [18]. The primary anthropogenic sources of methane are landfills and dumps, which could emit up to 2% (volume/volume) of methane in the atmosphere [19]. Considering the flammability of this hydrocarbon gas even in low concentrations as 5% [20], remote sensing and concentration measurement of this gas around those areas is indispensable [21].

The results of remote sensing experiments inside the laboratory motivated us to further develop experiments for the detection of trace methane in the open field using a spectroscopic LIDAR technique. The portable terawatt laser system designed by the Defence R&D Canada-Valcartier (DRDC-Valcartier), the *T&T Lab* [22], was successfully used for the experiment.

2. Experiment setup

The *T&T Lab* is a terawatt laser mounted in standard 20 ft sea container. This system is similar in many respects to Teramobile, the Franco-German laser system [23]. The laser system consists of a compact Ti:Sapphire laser oscillator and a chain of Ti:Sapphire amplifiers. The amplifier chain includes a regenerative amplifier and multipass amplifier pumped with a doubled Nd:YAG laser in the repetition rate of 10 Hz. The compressed pulse's spectrum is centered at 805 nm with a 25 nm bandwidth (FWHM). The pulse energy of the beam could be increased stepwise up to 100% (270 mJ/pulse) in 1% increments with a motorized variable attenuator. Minimum pulse duration was 45 fs. One compressor grating, mounted on a motorized translation stage, allows control of pulse width and eventual introduction of a negative chirp to pre-compensate for propagation dispersion of the beam over long distances.

The experiment was performed in a 60-m long outdoor corridor with the same experimental setup used in the laboratory. A schematic of the setup is shown in Fig. 1. The laser pulses were prechirped negatively to 5 ps in the compressor with two energy values used: 110 and 190 mJ per pulse. A telescopic system (focusing beam expander), which consisted of a 50 mm diameter convex mirror (M2) with a focal length of 50 cm and a 80 mm diameter

* Corresponding author.
E-mail address: yousef.kamali.1@ulaval.ca (Y. Kamali).

0030-4018/$ - see front matter © 2009 Elsevier B.V. All rights reserved.
doi:10.1016/j.optcom.2009.02.017

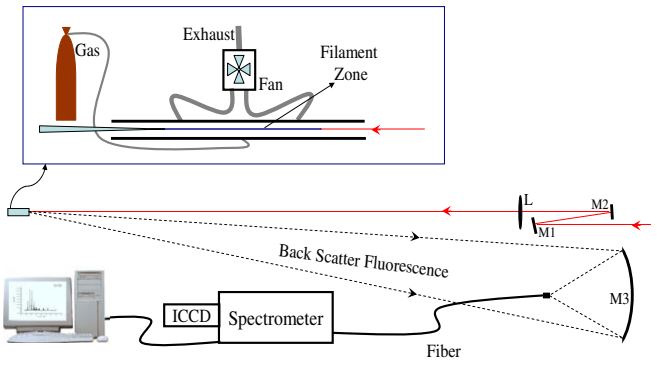

Fig. 1. Experimental setup. M1: zero degree 800 mirror; M2: convex mirror with $f = 50$ cm focal distance; L: lens with $f = 100$ cm; M3: LIDAR mirror with $f = 1.5$ m, the diameter $D = 25$ cm. The fluorescence signal was collected and focused into a fiber which was connected to spectrometer and ICCD. The distance between L and M1 was variable. The distance between the 2 m metal tube (target) and the LIDAR mirror was 22 m in the laboratory, 10 and 20 m in the field. The metal tube was connected to the gas cylinder and exhaust.

plano-convex lens (L) with a focal length of 100 cm, was used to create and locally control filaments at long distances [24].

The gas mixture was flowed inside a 2-m long, open-ended stainless steel pipe of 76 mm diameter. The design of this open cell, as opposed to a sealed one, eliminated the reflected white-light SC from the windows and the generation of white-light inside the windows. It also avoided the damage of the windows since the length of the filament could be longer than the pipe and interact with the windows of a sealed gas cell. The open cell was located at 10 and 20-m away from the telescope and the detector. The location of the filament was positioned around the center of the open cell at both locations. The balanced gas mixture of 2% methane with air was fed into the open cell in a flowing state using few tens meter long plastic tubes and output pressure of 40 psi on the gas regulator. Subsequently the gas mixture was forced out of the pipe through a fan and exhaust line. The backscattered fluorescence was collected by a LIDAR system with an aluminum mirror (M3: focal length 1.5 m and diameter 25 cm) and then focused onto the fiber bundle, which was connected to the spectrometer and ICCD.

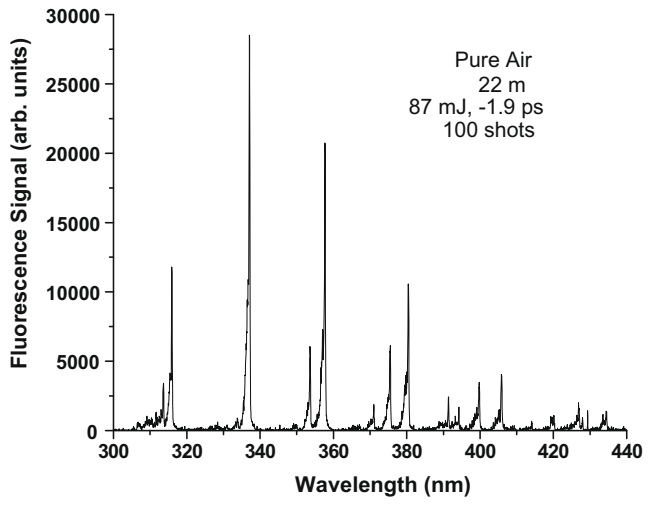

Fig. 2. Filament-induced fluorescence spectra (FIFS) of ambient air at the pressure of 1 atm inside the laboratory for 22 m distance between filament zone and LIDAR mirror and 100 shots of accumulation with the 87 mJ and (-chirped)1.9 ps laser pulses.

3. Results and discussion

Fig. 2 shows typical time-resolved filament-induced fluorescence spectra (FIFS) of ambient air at a pressure of 1 atm inside the laboratory. The vertical axis is ICCD counts numbers which are proportional to the fluorescence signal and the horizontal axis

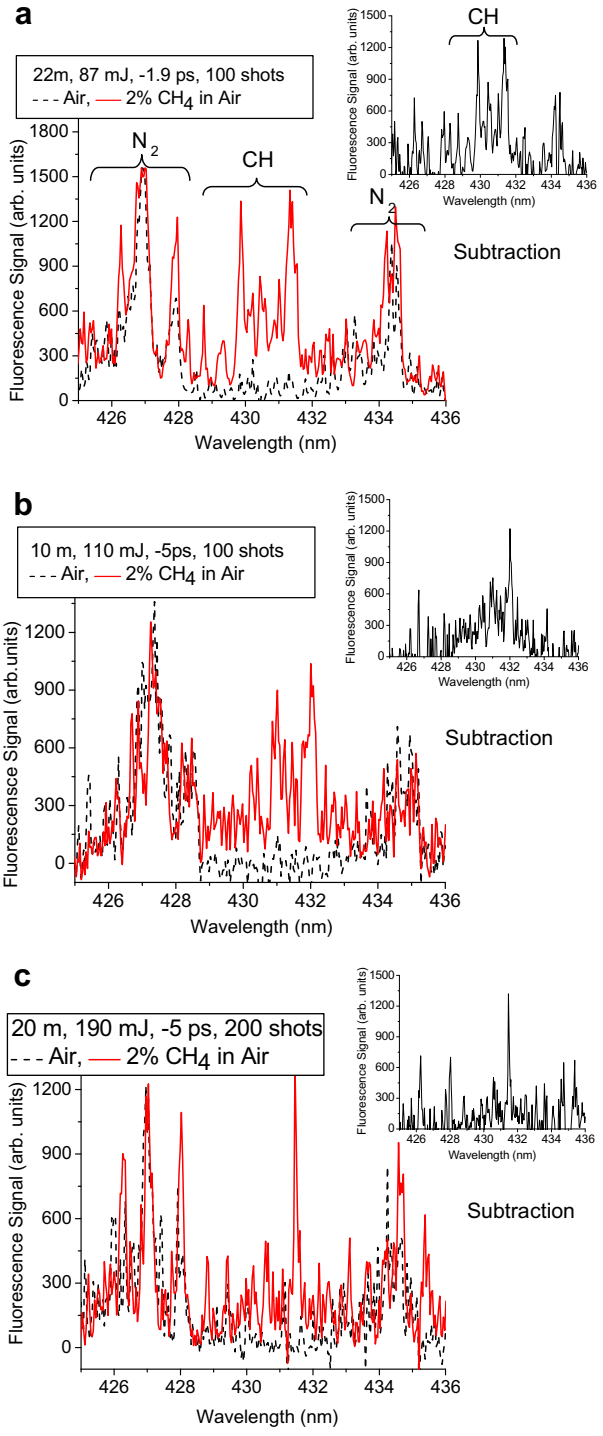

Fig. 3. (a) The spectra of pure air (black-dashed) and contaminated air with 2% methane (red in web and black in print version) for 22 m distance between the target and LIDAR mirror inside the laboratory. Inset: the subtraction of two spectra. In the field, (b) the fluorescence signal of methane for 10 m distance using 110 mJ per pulse with (-chirped) 5 ps and 100 shots of accumulation and (c) The fluorescence signal of methane for 20 m distance using 190 mJ per pulse with (chirped) 5 ps and 200 shots of accumulations.

shows different wavelengths in units of nanometer. This spectrum was taken when the distance between the gas target and LIDAR mirror was 22 m. The spectrum is an accumulation of 100 shots of the 87 mJ laser pulses with the pulse duration of 1.9 ps (negatively chirped). It benefits also from setting on the ICCD a proper temporal gate-width and gate-delay. The gate-width of the ICCD is optimized to 30 ns and this gate is opened when the laser pulse arrives at the interaction zone. The spectrum in Fig. 2 represents the fluorescence emission of nitrogen molecules in one atmosphere air [11]. The strongest peak is around 337 nm which is used for the primary alignment of the LIDAR system. When the air is contaminated by traces of methane, we expect to see CH fragment fluorescence peak around 430 nm as a finger print. There is no nitrogen peak around this wavelength that could potentially mask the CH peak. However, if there were some N_2 peaks that could cover the CH peak, we could use the gating technique to remove the N_2 signal considering the shorter lifetime of nitrogen fluorescence emission with respect to that of CH [15].

The spectra of pure air (black-dashed) and contaminated air with 2% methane (red in web and black in print version), shown in Fig. 3a, were captured from a distance of 22 m. Some peaks around 430 nm show the existence of methane. These peaks belong to different molecular transitions $A^2\Delta$–$X^2\Pi$ of CH radical which is produced from the dissociation of methane [25]. The fluorescence signal of CH band around 430 nm is clearly obtained by subtraction of the two spectra (inset of Fig. 3a).

Using DRDC-Valcartier's facilities, we repeated the same procedures as in the laboratory. The negatively chirped laser pulses of 110 mJ were being shot into the open field and the filaments were controlled at long distances by modifying the focusing condition of the telescope. Fig. 3b shows the fluorescence signal of the mixed sample captured from a 10 m distance using 110 mJ pulse energy, a −5 ps pulse duration and accumulated for 100 shots. For the longer distance of 20 m, the signal was weaker. In order to improve the signal strength, the laser energy and the number of shots were increased to 190 mJ and 200 shots, respectively (Fig. 3c). The insets of Fig. 3b and c show the subtraction of pure and contaminated air spectra.

For all the results, the peak power of the laser pulses used varied between $4.4P_{cr}$ to $9.2P_{cr}$. The critical power P_{cr} is 5GW for long pulse durations [26]. Although the plasma density inside the filament can vary depending on the initial peak power and pulse duration, it is still possible to compare the results. By taking into account the LIDAR equation correction factor ($1/D^2$, where D is the distance), the fluorescence strength measured (F_s), the number of shots accumulated (S) and the peak power of the laser (P in terms of P_{cr}), we can express the signal strength as a "corrected" fluorescence signal (F_{corr}). The gain of the ICCD was the same for all the experiments, and assuming that the collection efficiency of the LIDAR was the same for both the laboratory and the field experiments, we can consider these parameters as being fixed. In the case of the peak power, we assume that the amount of fluorescence is proportional to the peak power because the number of filaments is usually considered to increase directly with the peak power while intensity clamping fixes the laser intensity inside the filaments. We can therefore use the so-called corrected fluorescence signal (F_{corr}) to compare the signal given by:

$$F_{corr} = \frac{F_s D^2}{SP}$$

All parameters of F_s, D, S, P and F_{corr} are compared for both the laboratory and field results of methane detection (Table 1). On the basis of comparison, the efficiency to detect the CH fluorescence is decreased by a factor of only three to four between the laboratory experiment and the field experiments. Considering the strong effect of the atmospheric turbulence on the filamentation process [27], the asymmetric profile of the laser beam used for the outdoor experiments and the varying sunlight background that by experience has a strong effect on the sensors, these results are very encouraging. They validate our long range extrapolation techniques on the results obtained in the laboratory.

The laser beam quality is one of the factors explaining the discrepancy between the results of the laboratory and field experiments. The different beam patterns obtained in the laboratory and in the field after the focusing beam expander (telescope) are presented in Fig. 4. There is a clear difference between the two beam patterns. The laser beam in the laboratory is more symmetric and centric. More systematic experiments should be done for a quantitative analysis about the contribution of all these three factors: the beam quality, the sunlight background and the air turbulence. For example a sophisticated turbulent air chamber could be designed inside the laboratory to measure the influence of air turbulence on the backscattered fluorescence signal.

Table 1
Comparison of parameters in the laboratory and the field experiments. F_s: the fluorescence strength, D: the distance, S: the number of accumulation shots, P: the peak power of the laser in term of P_{cr} and F_{corr}: corrected fluorescence signal.

	Fig. 3a (lab)	Fig. 3b (DRDC)	Fig. 3c (DRDC)
F_s, integrated value (428.5–432 nm)	1675.5	1226.4	749.8
D	22 m	10 m	20 m
S	100 shots	100 shots	200 shots
P	$9.2P_{cr}$	$4.4P_{cr}$	$7.6P_{cr}$
F_{corr} (counts m^2/shot P_{cr})	879.6	278.5	197.1

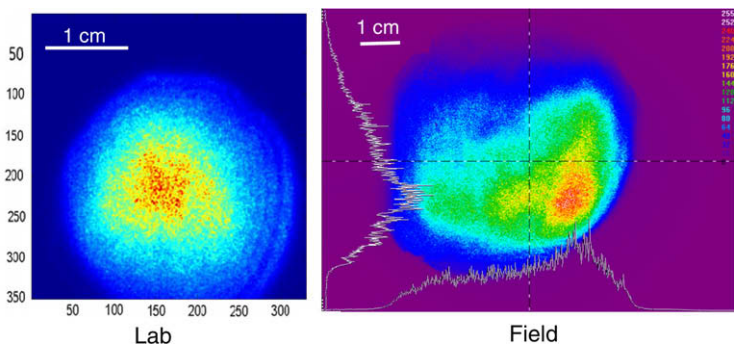

Fig. 4. The beam pattern after focusing beam expander (telescope) in the laboratory and the field.

4. Conclusion

The outdoor remote sensing of trace methane using filament-induced fluorescence in air is reported. From the comparison of the results of the laboratory and the field, it seems that the "deterioration" of the filamentation from the atmospheric turbulence, the profile of the laser beam, combined with the varying sunlight background decreased the efficiency to detect the CH fluorescence by a factor of only three to four between the laboratory experiment and the field experiment. This conclusion justifies the extrapolations of the results obtained in the laboratory to longer ranges. Thus, the current result could be considered a breakthrough in remote sensing based on filamentation.

More systematic experiments should be done for giving a precise analysis about the contribution of the air turbulence and beam quality on filamentation.

Acknowledgements

This work was partially supported by NSERC, DRDC-Valcartier, University of Mohaghegh Ardebili, Canada Research Chairs, CFI, FQRNT and CIPI. Technical support and assistants of M. Martin, M. Jean and M. Cardinal are highly appreciated.

References

[1] A. Couairon, A. Mysyrowicz, Phys. Rep. 441 (2007) 47.
[2] S.L. Chin, S.A. Hosseini, W. Liu, Q. Luo, F. Théberge, N. Akozbek, A. Becker, V.P. Kandidov, O.G. Kosareva, H. Schroeder, Canadian Journal of Physics 83 (2005) 863.
[3] A. Couairon, S. Tzortzakis, L. Berge, M. Franco, B. Prade, Andre Mysyrowicz, J. Opt. Soc. Am. B 19 (2002) 5.
[4] A. Ting, I. Alexeev, D. Gordon, R. Fischer, D. Kaganovich, T. Jones, E. Briscoe, J. Peñano, R. Hubbard, P. Sprangle, Phys. Plasmas 12 (2005) 056705.
[5] F. Théberge, W. Liu, P.T. Simard, A. Becker, S.L. Chin, Phys. Rev. E 74 (2006) 036406.
[6] Y.P. Deng, J.B. Zhu, Z.G. Ji, J.S. Liu, B. Shuai, R.X. Li, Z.Z. Xu, F. Théberge, S.L. Chin, Opt. Lett. 31 (2006) 546.
[7] H.R. Lange, A. Chiron, J.-F. Ripoche, A. Mysyrowicz, P. Breger, P. Agostini, Phys. Rev. Lett. 81 (1998) 1611.
[8] J. Kasparian, R. Sauerbrey, S.L. Chin, Appl. Phys. B 71 (2000) 877.
[9] A. Becker, N. Akozbek, K. Vijayalakshmi, E. Oral, C.M. Bowden, S.L. Chin, Appl. Phys. B 73 (2001) 287.
[10] W. Liu, S. Petit, A. Becker, N. Akozbek, C.M. Bowden, S.L. Chin, Opt. Commun. 202 (2002) 189.
[11] A. Talebpour, M. Abdel-Fattah, A.D. Bandrauk, S.L. Chin, Laser Phys. 11 (2001) 68.
[12] Q. Luo, S.A. Hosseini, B. Ferland, S.L. Chin, Opt. Commun. 233 (2004) 411.
[13] J.-F. Gravel, Q. Luo, D. Boudreau, X.P. Tang, S.L. Chin, Anal. Chem. 76 (2004) 4799.
[14] H.L. Xu, J.F. Daigle, Q. Luo, S.L. Chin, Appl. Phys. B 82 (2006) 655.
[15] H.L. Xu, Y. Kamali, C. Marceau, P.T. Simard, W. Liu, J. Bernhardt, G. Méjean, P. Mathieu, G. Roy, J.-R. Simard, S.L. Chin, Appl. Phys. Lett. 90 (2007) 101106.
[16] A. Iwasaki, N. Aközbek, B. Ferland, Q. Luo, G. Roy, C.M. Bowden, S.L. Chin, Appl. Phys. B 76 (2003) 231.
[17] Q. Luo, H.L. Xu, S.A. Hosseini, J.-F. Daigle, F. Theberge, M. Sharifi, S.L. Chin, Appl. Phys. B 82 (2006) 105.
[18] P.L. Hanst, S.T. Hanst, in: M.W. Sigrist (Ed.), Air Monitoring by Spectroscopic Techniques, Wiley, New York, 1994, p. 1.
[19] M. Héry, A.C. Singer, D. Kumaresan, L. Bodrossy, N. Stralis-Pavese, J.I. Prosser, I.P. Thompson, J.C. Murrel, ISME J. 2 (2008) 92.
[20] <http://www.toxicsites.org/Explosions_And_Fires_At_Dumps.pdf>.
[21] National AG Safety Database (NASD); See <http://www.cdc.gov/nasd/docs/d001001-d001100/d001097/d001097.html>.
[22] M. Châteauneuf, J. Dubois, SPIE, doi: 10.1117/2.1200612.0506 <https://spie.org/x8496.xml?highlight=x2404>.
[23] H. Wille, M. Rodriguez, J. Kasparian, D. Mondelain, J. Yu, A. Mysyrowicz, R. Sauerbrey, J.P. Wolf, L. Wöste, EJP Appl. Phys. 20 (3) (2002) 183.
[24] W. Liu, F. Théberge, J.-F. Daigle, P.T. Simard, S.M. Sarifi, Y. Kamali, H.L. Xu, S.L. Chin, Appl. Phys. B85 (2006) 55.
[25] F. Kong, Q. Luo, H. Xu, M. Sharifi, D. Song, S.L. Chin, J. Chem. Phys. 125 (2006) 133320.
[26] W. Liu, S.L. Chin, Opt. Express 13 (2005) 5750.
[27] A. Houard, M. Franco, B. Prade, A. Durécu, L. Lombard, P. Bourdon, O. Vasseur, B. Fleury, C. Robert, V. Michau, A. Couairon, A. Mysyrowicz, Phys. Rev. A 78 (2008) 033804.